Measurements of leakage, structural stiffness and energy dissipation parameters in a shoed brush seal

By Adolfo Delgado and Luis San Andrés (Texas A&M University), and John F Justak (Advanced Technologies Group Inc, Stuart, Florida), USA

The shoed brush seal is a modification of a standard brush seal that has a number of arcuate pads at the free ends of the bristles. A major benefit of this novel design is that it allows reverse shaft rotation. It also eliminates bristle wear as the pads lift off due to the generation of a hydrodynamic film during rotor spinning. This type of seal, able to work at both low and high temperatures, not only restricts secondary leakage but also acts as an effective vibration damper. The dynamic operation of the shoed-brush seals, along with the validation of reliable predictive tools, relies on the correct estimation of the seal structural stiffness and energy dissipation features. This article describes tests to measure these parameters and compare the results with predictions.

Nomenclature

A = Shaft cross-sectional area (127 mm^2)
A_u = Seal area upstream [m^2]
= $(\pi/4)*(D_u^2-D_j^2)$
B = Brush seal effective film thickness [m]
c_E = Equivalent 'labyrinth seal' clearance [m]
C_{eq} = System equivalent viscous damping coefficient [N.s/m]
E_{dis} = Energy dissipated in one period of forced motion [J]
F_{ext} = Excitation force [N]
K_{eq} = Equivalent stiffness for test system [N/m]
K_{shaft} = Shaft stiffness [N/m]
K_s = Brush seal structural stiffness
L = Shaft length [0.248 m]
m = Seal leakage [g/s]
M_{eq} = System equivalent mass [kg]
M_D = Disk mass [1.36 kg]
p_r = Pressure ratio, P_u/P_d
P_u, P_d = Upstream (supply) and downstream (discharge) absolute pressures [Pa]
r = Frequency ratio, ω/ω_n
t = Time [s]
T_u = Upstream (supply) temperature [°C]
x = Displacement [m]
z = Axial coordinate along shaft [m]
γ_{eq}, γ_s = Structural loss coefficients, equivalent and brush seal
γ = Gas ratio of specific heats
μ = Brush seal dry friction coefficient
ρ = Shaft density (7800 kg/m^3)
Φ = Brush seal flow factor
φ = Equivalent orifice flow factor for a brush seal
$\psi(z)$ = Shape function of cantilever beam due to a static load
ω = Excitation frequency [rad/s]
ω_n = System natural frequency [rad/s]
= $(K_{eq}/M_{eq})^{1/2}$

Complex variables:
F = Synchronous component of force
X = Synchronous component of displacement
Z = Impedance function, F/X

Subscripts:
eq = Equivalent system: shaft + disk + brush seal
f = Measurement axial location, load action
s = Seal and disk axial location

Introduction

Improvements in air-breathing turbomachinery efficiency can be realized with reliable, and predictable, sealing technology. Brush seals have better leakage performance than labyrinth seals,[1] require less axial space and are also able to handle larger vibrations.[2] Furthermore, experimental evidence shows that brush seals exhibit favorable rotordynamic characteristics when compared to labyrinth seals.[3, 4] However, premature wear and limitations in sealing pressure differentials have confined brush seals to hybrid configurations, where brush seals are intercalated between labyrinth seals.[5] These configurations take advantage of the seals' superior leakage performance, but not the axial space reduction and favorable vibration characteristics associated with brush seals. Furthermore, a brush seal can accommodate shaft rotations in only one direction, thus preventing use in certain aircraft engine applications.

Justak[6] introduced a novel brush seal design that incorporates metal pads at the free end of the bristles (**Figure 1**). This modification allows reverse shaft rotation and also significantly reduces or eliminates bristle wear, since each individual pad lifts due to a hydrodynamic fluid film wedge induced by rotor spinning. The non-contact compliant seal gap is maintained through a combination of hydrodynamic pressure and balanced hydrostatic pressures. Justak[7] also presented very favorable leakage performance compared with a standard brush seal. Delgado *et al.*[8] have presented a model and measurements to determine the static structural stiffness coefficient of shoed brush seals. The experiments showed evidence of hysteresis caused by dry friction from bristle-to-bristle and bristle-to-back plate interactions.

Delgado *et al.*[9] have also presented an analysis for prediction of the rotordynamic force coefficients in a shoe-brush seal. The model couples the gas film forces generated in the thin gap between the rotor and a shoe and the structural characteristics, stiffness

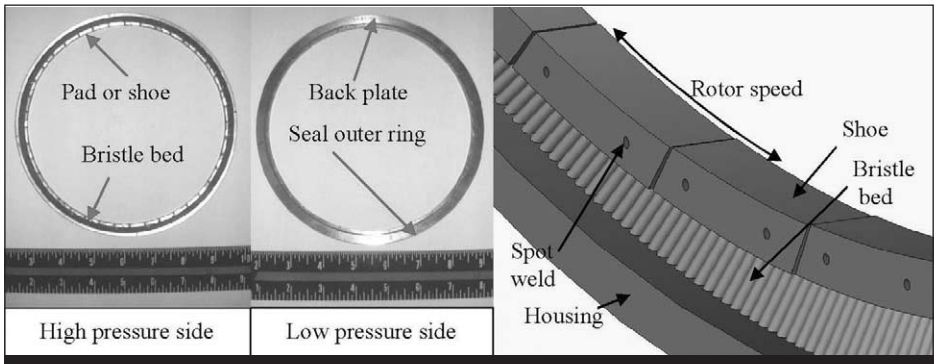

Figure 1. A shoed-brush seal and close-up schematic view.

and damping, from the bristle bed underneath. The predictions indicate that the overall stiffness and damping coefficients in a shoed brush are not affected by either the operating gas film clearance or the supply to discharge pressure ratio. On the other hand, direct stiffness drops rapidly with increasing operating shaft speeds. The predictions for damping rely on the appropriate physical characterization of the energy dissipation in the bristle bed, and are modeled as an empirical structural loss factor.

A test rig to measure leakage and to perform dynamic load tests in brush seals is described, together with a simple identification method to extract the seal structural stiffness and damping parameters. The test data, needed to validate predictive models of brush seal performance, bring forward this novel seal technology.

Test rig description

Figure 2 shows a cross-section view of the test rig. A long and slender steel shaft, 12.7 mm in diameter, and an aluminum disk mounted at the shaft end are located inside a cylindrical, thick wall, steel vessel. The disk diameter and thickness are 163 mm and 25.4 mm, respectively. One end of the shaft is affixed into the bottom of the vessel with two rolling element bearings. The test brush seal is secured at the top of the vessel with an interference fit to the disk.

Thus, the simple test system comprises a cantilever beam whose free end carries a large inertia, disk and the test seal element, which offers stiffness and damping connections to ground. The cylindrical vessel can be pressurized to conduct leakage measurements through the test seal.

A piezoelectric load cell and long stinger connect the end of the shaft to an electromagnetic shaker, softly supported from rubber cords. Two small brackets, 90° apart, are mounted on the outer diameter of the solid disk. Two eddy current sensors on the top of the vessel, facing the brackets, record the disk displacements. Two piezoelectric accelerometers, attached to the brackets, record the disk acceleration along two orthogonal directions on the horizontal plane. **Table 1** lists the dimensions and material properties of the test brush seal.

Static and dynamic load experiments to characterize the structural properties of the test seal were conducted with no shaft rotation and at room temperature (23°C). The test system is modeled with one degree of freedom (1-DOF). The equivalent stiffness K_{eq} and mass M_{eq} are determined at location L_f, where the external load is applied, and displacements and accelerations are recorded. The system equivalent stiffness and mass comprise various elements where K_{shaft} (= 54 kN/m) and K_s represent the shaft and brush seal stiffnesses, respectively; M_D is the aluminum disk mass (1.36 kg); and ρ and A denote the shaft material density and cross-sectional area, respectively.

Impact loads and static, pull loads exerted on the disk before installing the brush seal aim to identify the baseline parameters of the test rig. The static load experiments involve pulling the disk with calibrated weights through a rope-and-pulley system and recording the shaft deflection. The natural frequency of the shaft and disk alone is 33 Hz, and was measured by a impact hammer hit to the disk and recording the ensuing disk motions. The displacement/load transfer function leads to a shaft stiffness (K_{shaft}) of 52 kN/m and a system mass (M_{eq}) of 1.18 kg. The shaft stiffness derived from the static load tests is 53.4 kN/m. The system motion due to the impacts shows a very small damping ratio ~0.001.

The brush seal was installed with an assembly diametral interference with the disk of 0.890 mm. Impact load tests show that the damped natural frequency of the system increases to 53 Hz and the disk motions are well damped. The brush seal stiffens the system and adds substantial damping. Static load tests with the brush seal in place were conducted for multiple sets of pull loads.

These tests are divided into tapping and non-tapping, as used by Delgado *et al.*[8] The

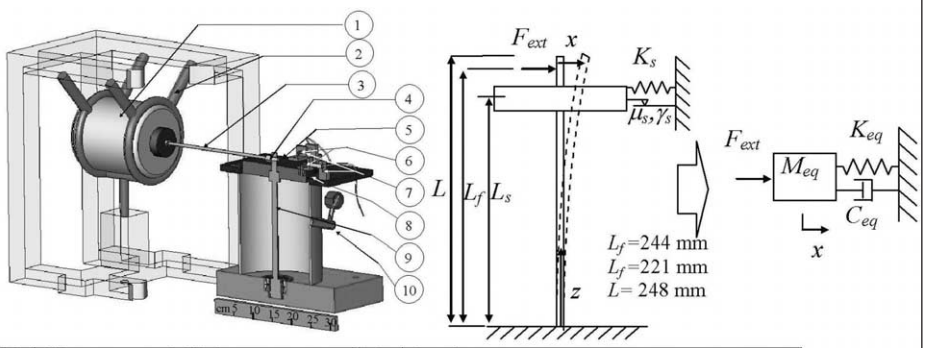

1	Electromagnetic Shaker	6	Accelerometers
2	Soft supports (rubber cords)	7	Targets and displacement sensors
3	Stinger	8	Shoed brush seal
4	Load Cell	9	Cantilever shaft
5	Solid Disk	10	Air inlet

Figure 2. Cross-sectional view of the brush seal test rig, and representation of the equivalent mechanical system.

Physical properties	Magnitude
Disk diameter	162.9 mm
Pad length	3.2 mm
Number of pads	20
Pad arc length	18°
Pad mass, m_P	1.34 g
Pad length	24.69 mm
Bristle diameter, d_b	0.05334 mm
Bristle free length, L_b	10.114 mm
Bristle lay angle	42.5°
Bristle modulus of elasticity, E	22.48×10^5 bar
Bristle density (circumference)	1350 bristles/cm

Table 1. The geometry of the 20 shoe brush seal.

tapping and non-tapping on the seal disk demonstrate the effects of dry friction and hysteresis arising from the bristle-to-bristle interactions. Thus, two limiting values of test system static stiffness (K_{eq}) are estimated at 125 (±4) kN/m and 176 (±7) kN/m for the tapping and non-tapping conditions, respectively. The resulting range of static stiffness for the brush seal alone (K_s) as derived from the equivalent system stiffness magnitude is 100 to 170 (±8) kN/m, and which encloses the value of seal stiffness obtained from dynamic load tests (132 kN/m), as determined below.

Results from dynamic load tests

Single frequency dynamic load tests were conducted, from 25 to 100 Hz, and for four force magnitudes. Tests at frequencies below 25 Hz were not performed, to avoid the influence of the shaker soft mount natural frequency at ~10 Hz. The maximum force amplitude, 48 N, was set to avoid exceeding the assembly interference of 0.89 mm for excitations at the system natural frequency, thus avoiding loss of contact between the brush seal shoes and disk. The lowest force, 35 N, is the minimum to induce measurable disk motions, *i.e.* the force necessary to overcome the inherent dry friction of the test seal element. Additional experiments with an intermediate force amplitude, 44 N, were conducted over a wider frequency range extending from 30 Hz to 300 Hz.

Figure 3 shows the disk amplitude of motion synchronous with the frequency of the applied load. The amplitude of applied load remained fixed while the frequency was varied. There is a threshold force of less than 40 N, below which the system does not show a resonance peak at the damped natural frequency of 53 Hz. The threshold force relates to the transition from a stick-slip motion regime into a macro slip regime.

For the large load, 48 N, the disk motions are also large and mainly synchronous with the excitation frequency. On the other hand, at 35 N load the motion amplitudes are considerably smaller, up to 75%, and do not evidence a resonance peak as is apparent for the two largest loads. For the low loads, the disk motion is in a nonlinear micro stick-slip regime, where the dry friction force is not constant. As the load amplitude increases, the seal response transitions into a macro-slip regime, where the motion is linear and the friction force is nearly constant in amplitude. Importantly enough, for load amplitudes of 44 N and 48 N, the recorded displacements show a nonlinear effect since at the resonant frequency, a difference in the load of just 4 N produces a large change (0.30 mm) in the amplitude.

Parameter identification procedure

The applied force is periodic and the seal motion (x) is of identical frequency for motions recorded for loads of magnitude larger than 44 N, which permits calculation of the complex impedance (**Z**) function. The test system stiffness (K_{eq}) and mass (M_{eq}) are readily obtained from $K_{eq} - M_{eq}\omega^2 = \mathrm{Re}(\mathbf{Z})$ over a pre-defined frequency range.

The motion of the brush bristles under bending and the dry friction arising from bristle-to-bristle and bristles-to-back plate interactions causes the seal dynamic forced response. The energy dissipation mechanism is clearly not of the viscous type. Presently, the energy dissipation model comprises structural and dry friction damping mechanisms. The energy dissipated in one period of seal motion can then be calculated.

Figure 4 depicts the recorded and model derived amplitude of response versus frequency. The force of magnitude 48 N is kept constant throughout the frequency span. The model predictions use the identified system parameters given in **Table 2**. **Figure 5** depicts the energy dissipated by the test system in one period of motion and increasing frequencies to 300 Hz. The identified parameters render accurate predictions over a broad frequency rage, *i.e.* 30 Hz to 200 Hz. The shaded area above 240 Hz encloses the second natural frequency of the test rig system. Thus, the identified dry friction (μ) and structural loss (γ) coefficients are rather independent of excitation frequency.

Seal leakage measurements

Measurements of leakage through the test seal were conducted for increasing air pressures at ambient conditions. Recall that these measurements are without shaft rotation. The measured flow rates are correlated to predictions based on a semi-empirical leakage model advanced by Chupp and Holle.[10] An Excel VB program contains this model.[11] The upstream pressure range increased from 1.01 to 3.25 bar. A turbine flowmeter and strain gauge sensor record the flow rate and upstream pressure measurements, respectively.

Figure 6 presents the measured leakage or mass flow rate (m) versus the pressure ratio ($p_r = P_u/P_s$) and the leakage flow model predictions using a uniform effective thickness B = 0.437 mm (0.017 inch). The effective thickness (B) is an empirical parameter that the model relies on. The selected B renders best correlation to the experimental data at $p_r \sim 2.5$.

Brush seal manufacturers (see, for example, Reference 7) also characterize brush seal leakage

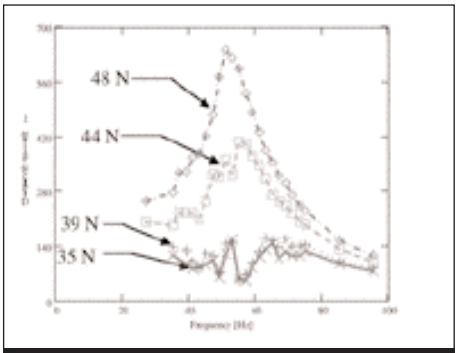

Figure 3. Measured amplitude of motion (|X|) synchronous with dynamic load excitation frequency. Test load magnitudes are indicated.

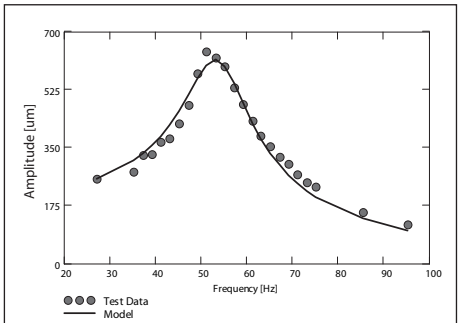

Figure 4. Amplitude of synchronous motion versus frequency. Load magnitude = 48 N. Correlation of model predictions to test results.

Parameters	Equivalent system	Brush seal alone
Stiffness, kN/m	143	132
R^2	0.99	–
Dry friction coefficient, μ	–	0.55
Loss factor coefficient, γ	0.16	0.19
R^2	0.97	–

Table 2. Test system and brush seal identified parameters from dynamic load tests, with load of 48 N, at 25–95 Hz.

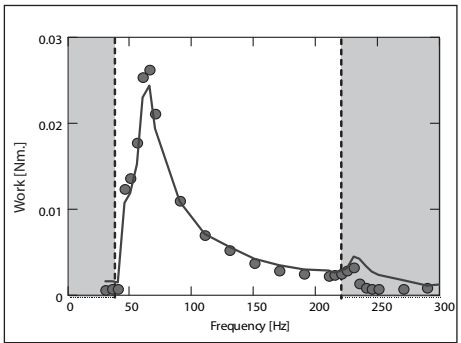

Figure 5. Work = energy dissipated by test system versus frequency for one period of motion. External load is 44 N in the frequency range 30–300 Hz.

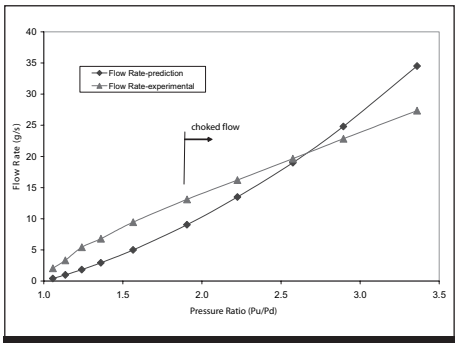

Figure 6. Measured and predicted leakage for test shoed brush seal versus pressure ratio. Predictions based on uniform effective thickness B = 0.437 mm.

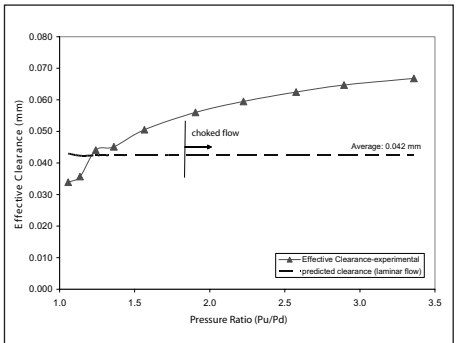

Figure 7. Equivalent labyrinth seal clearance for test brush seal, from leakage measurements and predictions based on laminar flow model c_E = 0.042 mm.

performance in terms of an effective clearance (c_E) that represents a film thickness equivalent to that of a corresponding 'one sharp tooth' labyrinth seal.

Figure 7 shows the calculated effective 'labyrinth seal' clearance and predictions derived from the laminar flow model versus pressure ratio. The average predicted clearance is 0.042 mm (0.0016 inch), while the one derived from the flow measurements increases to 0.067 mm (0.00263 inch) at the highest pressure tested. Note that the shoed brush seal shows a 200% increase in effective clearance over the pressure range tested. The change is due to the 'opening' of the seal pads as they are pushed away from the shaft as the pressure upstream increases.

Conclusions

Experimental results and a procedure for estimation of the structural stiffness and damping characteristics of a 20-pad shoed brush seal have been presented. The simple test rig comprises a non-rotating cantilever shaft with a solid disk at its free end. The test seal static structural stiffness is not unique, since it depends on whether the procedure allows for stick or slip to occur. The stick/slip is due to the bristle-to-bristle and bristles-to-back plate dry friction interactions.

In the dynamic load tests, a force of a certain magnitude is needed to overcome the stick/slip. In the identification procedure conducted in the frequency domain, the stiffness and mass coefficients are readily obtained from the real part of the system impedance. The brush-seal energy dissipation mechanism is modeled as a combination of structural and Coulomb damping, and is represented by a structural loss factor (γ_s) and a dry friction coefficient (μ), respectively. These parameters are identified in the frequency range from 25 Hz to 95 Hz, enclosing the test system natural frequency of 53 Hz. Model predictions based on the identified parameters (γ_s = 0.55, μ = 0.19) reproduce the measured amplitude of motion and energy dissipated, even for frequencies higher than the largest in the identification range.

Seal leakage measurements for increasing supply pressures show a unique performance characteristic, *i.e.* very small flow rate, effectively represented as a labyrinth seal of very narrow clearance. Empirical characterization of the shoed brush seal energy dissipation features is crucial for predictions and validation of its rotordynamic coefficients.

Acknowledgments

Thanks to the TAMU Turbomachinery Research Consortium for funding the work, and to Mr John Justak from Advanced Technologies Group Inc (641 SE Central Parkway, Stuart, FL 34995, USA, www.advancedtg.com), the originator of the concept, for providing the test seal.

References

1. R. Chupp, E. Raymond and P. Nelson: Evaluation of brush seals for limited-life engines, *AIAA J. Propulsion and Power*, **9**, 1995, 113–119.
2. J.A. Fellenstein and C. DellaCorte: A new tribological test for candidate brush seal material evaluation, *Tribology Transactions*, **39**, 1996, 173–179.
3. J.K. Conner and D. Childs: Rotordynamic coefficient test results for a four-stage brush seal, *AIAA J. Propulsion and Power*, **9**, 1993, 462–465.
4. D. Childs and J.M. Vance: Annular gas and rotordynamics of compressors and turbines. Proceedings of the 26th Turbomachinery Symposium, 1997, 201–220.
5. R.C. Hendricks, K.R. Csavina, T.A. Griffin, T.R. Kline, A. Pancholi and D. Sood: Relative comparison between baseline labyrinth and dual brush compressor discharge seals in a T-700 engine test. ASME Paper 94-GT-266, 1994.
6. J. Justak: Hybrid brush seal capable of reverse rotation. Proposal to US Navy SBIR Program, Advanced Turbomachinery Solutions, Stuart, Florida, 2000.
7. J. Justak: Hybrid brush seal capable of reverse rotation. Technical Report, Navy SBIR Phase II Project, Advanced Technologies Group Inc, Stuart, Florida, April 2002.
8. A. Delgado, L. San Andrés and J. Justak: Identification of stiffness and damping coefficients in a shoed brush seal. Proceedings of the VII Congreso y Exposición Latinoamericana de Turbomaquinaria, Veracruz, Mexico, October 2003.
9. A. Delgado, L. San Andrés and J. Justak: Analysis of performance and rotordynamic force coefficients of brush seals with reverse rotation ability. ASME Paper GT-2004-53614, 2004.
10. R.E. Chupp and G.F. Holle: Generalizing circular brush seal leakage through a randomly distributed bristle bed, *ASME J. Turbomachinery*, **118**, 1996, 153–161.
11. L. San Andrés: Analysis of performance and rotordynamic force coefficients of brush seals with reverse rotation ability. Final Report to Advanced Turbomachinery Solutions (ATS), March 2003.

For more information, contact:
Professor Luis A. San Andrés, Tribology Group Leader, Turbomachinery Laboratory, Mechanical Engineering Department, Texas A&M University, College Station, TX 77843-3123, USA. Tel: +1 979 862 4744, Email: Lsanandres@mengr.tamu.edu, Web: phn.tamu.edu/TRIBgroup

This feature article is based on a paper presented at the 4th EDF/LMS Poitiers Workshop on Advanced Topics and Technical Solutions in Dynamic Sealing, in Poitiers, France on 6 October 2005. The meeting was jointly organized by Electricité de France (EDF) and the School of Mechanics and Solids (LMS) of the Université de Poitiers. ***For more information on the papers presented this year and on future workshops, contact:*** *Dr Mihai Arghir, MdC–HDR– MS, Université de Poitiers, UFR Sciences SP2MI, Téléport 2, Boulevard Pierre et Marie Curie, BP 30179, F-86962 Futuroscope Chasseneuil Cedex, France. Tel: +33 5 4949 6540, Fax: +33 5 4949 6504, Email: workshop@lms.univ-poitiers.fr, Web: www-lms.univ-poitiers.fr*